A Theory-Guided Machine Learning Method for Cure Cycle Optimization to Minimize Process-Induced Deformations in Composites

Caleb Schoenholz; Navid Zobeiry

OFFICIAL CONFERENCE PUBLICATION

Proceedings of the American Society for Composites - Thirty-Eighth Technical Conference (2023)

https://doi.org/10.12783/asc38/36531

RELATED SUBSTANTIALLY EXTENDED JOURNAL ARTICLE

C. Schoenholz and N. Zobeiry, "An Accelerated Process Optimization Method to Minimize Deformations in Composites Using Theory-Guided Probabilistic Machine Learning," Composites Part A 176, 107842 (2024).

https://doi.org/10.1016/j.compositesa.2023.107842

ABSTRACT

One of the most prevalent challenges faced in aerospace manufacturing is the accurate prediction, control, and mitigation of residual stresses and resulting process-induced deformations (PIDs) in composites. Unwanted dimensional changes in composite parts can cause significant geometry mismatches during aerostructure assembly, leading to decreased throughput and a loss of structural performance. In recent decades, process simulation tools have been developed to facilitate predictions and mitigations of PIDs through process optimization as well as methods such as tool compensation. However, such numerical approaches often rely on time-consuming, expensive, and deterministic characterization and model-fitting techniques. As a result, simulation tools may be error-prone in industrial settings, making PID predictions unreliable. Therefore, manufacturers rely on labor-intensive methods, such as shimming, to compensate for geometry mismatches during the assembly process. This paper presents an alternative methodology to predict and minimize PIDs in composites without using process simulation. The proposed method is solely based on a limited amount of element-level experimental tests and theory-guided machine learning (TGML). Experimental methods include autoclave-curing of L-shaped laminates with different cure cycles and quantifying the resulting PIDs using laser profilometry. Probabilistic ML models are then built to correlate temperature cycles directly to PIDs using Gaussian Process Regression (GPR) guided by the closed-form theory available for PID predictions. Finally, the theory-guided ML models are iteratively calibrated using additional targeted tests specified by the GPR algorithm to efficiently converge on an optimal cycle that minimizes PIDs and satisfies cost specifications. The proposed ML-based approach is a generalizable probabilistic method to optimize process parameters and mitigate PIDs without using expensive process simulations or conducting exhaustive characterization experiments.

Caleb Schoenholz, Navid Zobeiry*

Materials Science & Engineering Department, University of Washington, 302 Roberts Hall, Box 352120, Seattle, WA 98195-2120, U.S.A.

*Corresponding author, navidz@uw.edu

doi.org/10.12783/asc38/36531

INTRODUCTION

The manufacturing of fiber-reinforced polymer composites inevitably leads to the formation of residual stresses and, often, process-induced deformations (PIDs) [1–4]. Residual stresses arise during autoclave processing and may be retained in composite parts due to various complex phenomena at the micro-, macro-, coupon-, and component-levels [1]. Upon curing and demolding of parts, some internal stresses may be released through deformations such as bending. For composite parts with angled geometries like L-shapes, this can lead to PIDs such as changes in the enclosed angle(s) (i.e., spring-in or spring-out) or warping of initially flat sections (i.e., warpage), as schematically shown in Figure 1 [5]. These PIDs can cause significant mismatches between components during the assembly of aerostructures, higher production costs, and reduced mechanical efficiency.

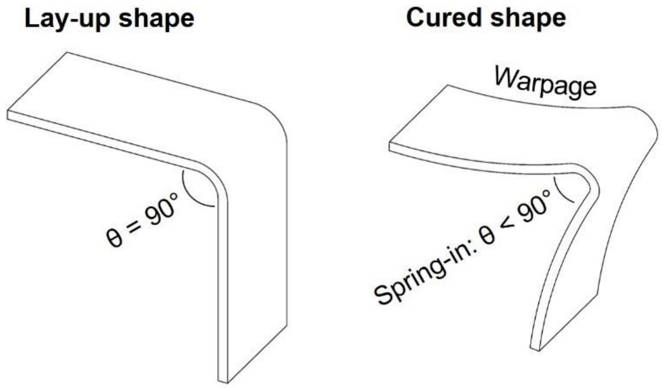

Figure 1. Schematic example of spring-in and warpage of an L-shaped composite part.

Despite having a general understanding of the contributing mechanisms of PIDs, manufacturers often lack confidence in predicting, controlling, and mitigating dimensional changes in industrial settings. Uncertainty in this regard partially arises from the challenges associated with characterizing and calibrating numerical models that are necessary for current physics-based simulation tools. For example, a simplified workflow to build and calibrate numerical models for predicting residual stresses and PIDs through process simulation includes the following steps. First, the composite's cure kinetics and thermo-mechanical properties must be experimentally characterized. Measuring these properties can be time-consuming, expensive, and challenging, particularly for complex structural material systems such as those used in the aerospace industry. Next, the measured properties are shaped into inputs for process simulation of composites using numerical modeling techniques. Typically, model-based or model-free fitting methods are deterministic and do not account for uncertainty associated with the composites manufacturing process or the limited amount of data generated during characterization. Calibration of the developed models is then performed, where the goal is to minimize the difference between predicted and experimental values. Trial-and-error, or deterministic methods such as least squares are often used for these processes, which also fail to account for the uncertainty associated with both the material and the manufacturing method. As a result, this process leads to inevitable errors in simulation predictions. Moreover, as the fidelity of simulation models increases, higher simulation and calibration costs are required, and the consequences for inaccurate simulation predictions are elevated. Thus, improving the previously described workflow or developing alternative approaches may be critical to help better understand and mitigate PIDs in composites.

This paper presents an alternative approach for predicting and mitigating PIDs in composites without the use of process simulation and time-consuming material characterization. The proposed method consists exclusively of limited numbers of coupon tests, combined with theory-guided machine learning (TGML) [6–10]. The experimental procedures involve autoclave-curing L-shaped laminates with different two-hold cure cycles and measuring the resulting PIDs. Then, probabilistic ML models are built to directly correlate temperature cycles with PIDs and manufacturing costs using Gaussian Process Regression (GPR) guided by closed-form theory available for PID predictions. Lastly, the TGML models are iteratively calibrated using additional targeted tests specified by the GPR algorithm to find the optimal cure cycle that reduces PIDs and satisfies cost constraints. The proposed ML-based approach is a probabilistic method for mitigating PIDs in composite parts without relying on expensive process simulation or conducting time-consuming characterization experiments.

EXPERIMENTAL

Material

The composite material used in this study was Toray T800S/3900-2B UD prepreg with a resin content of 35.5 % by weight [11]. 3900-2B is a toughened aerospace-grade epoxy resin, while T800S is an intermediate-modulus and high-strength carbon fiber. In addition to epoxy resin, the prepreg's surfaces are partially covered with micro-spherical thermoplastic tougheners. In recent decades, the T800/3900-2 system has been used as a primary structural material on major aircraft such as the Boeing 787 [12].

Laminate Manufacturing

Each experimental test in this study consisted of laying up three L-shaped composite parts with identical cross-ply stacking sequences and curing them in an autoclave. Three parts were fabricated during each experiment to account for and assess variability in the material and process. The configuration of each experiment is shown in Figure 2. To manufacture the parts, first, a custom-shaped tool made of 6.35 mm-thick A-36 steel was covered with one layer of fluorinated ethylene propylene (FEP) release film. Then, three L-shaped laminates consisting of eight plies of T800S/3900-2B were laid up, equally spaced across the width of the tool. Each L-shaped part had a flange length of 154.2 mm, a width of 50.8 mm, a corner radius of 15.875 mm, a corner angle of 90°, and a stacking sequence of $[0/90]_{2s}$. Next, the tool and composite laminates were covered with another sheet of FEP and one layer of breather cloth. The system was then sealed in vacuum bagging, loaded into an autoclave, and subjected to a specified cure cycle.

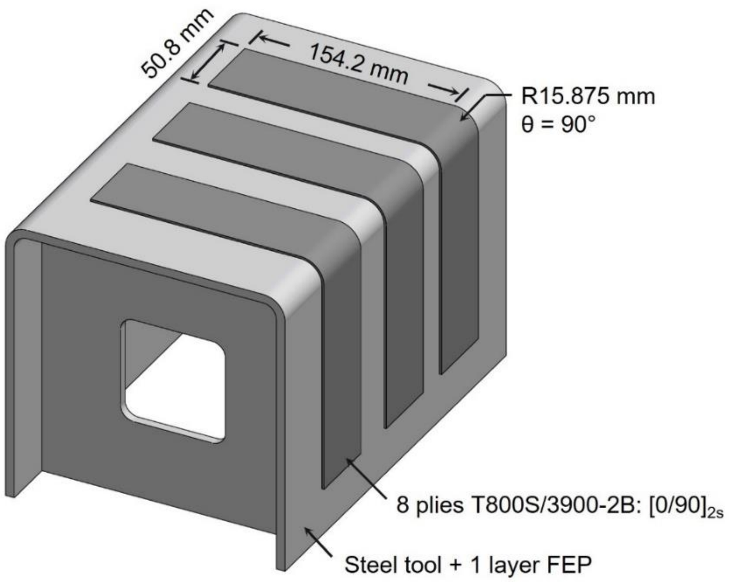

Figure 2. Experimental setup for manufacturing L-shaped composite parts.

PID Quantification

After each autoclave processing cycle, the cured L-shaped laminates were demolded from the tool and placed on their longitudinal sides. Then, a Keyence LJ-X8400 laser scanner was used to generate two-dimensional profiles in three locations spaced across the width of each part. Two profiles were scanned 6.25 mm away from each edge, and one profile was captured in the center of each flange, as schematically shown in Figure 3a. Next, each profile was superimposed on a plot containing the tool's two-dimensional profile. A custom Python [13] code was used to extract four values from the plot to quantify PIDs: corner spring-in, tip spring-in, maximum flange warpage, and deformation. Schematic representations of these values are shown in Figure 3b. Spring-in values denoted angles between the part and tool profiles at the flange corner ($\Delta\theta_{corner}$) and tip ($\Delta\theta_{tip}$), and maximum warpage (w_{max}) represented the highest out-of-plane flange deformation for each scan. Lastly, a deformation (δ) value was obtained by calculating the two-dimensional area between the tool and part profiles for each scan, then converting these areas to a single volumetric deformation value using piecewise numerical integration.

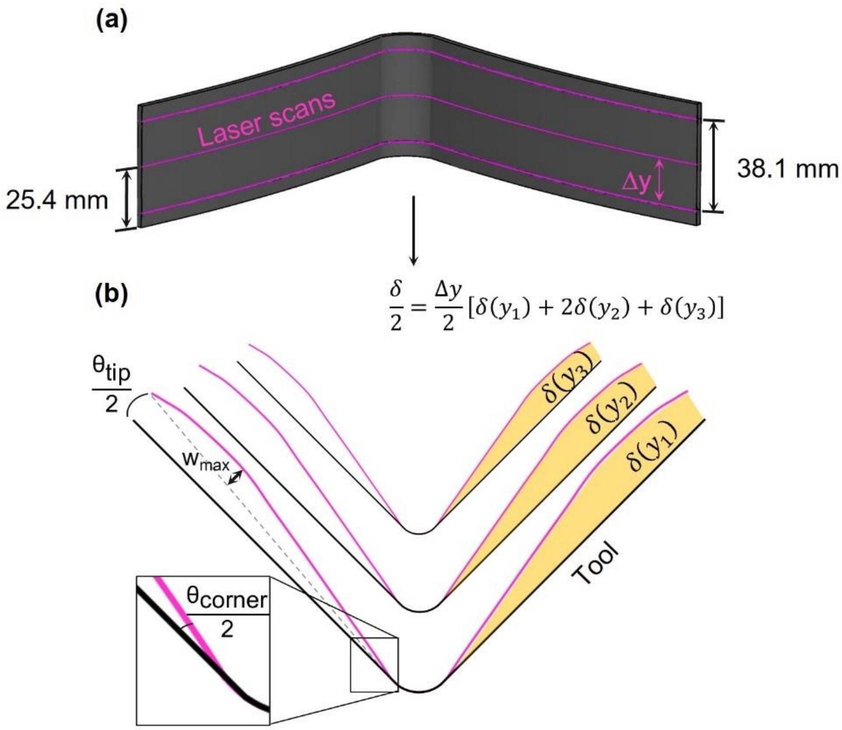

Figure 3. (a) Locations of laser scans for quantifying PIDs, (b) graphical definitions of corner spring in (θ_{corner}), tip spring-in (θ_{tip}), warpage (w_{max}), and deformation (δ) used in the present study.

TGML METHODOLOGY

In this section, a methodology is introduced to find an optimal cure cycle to minimize PIDs in L-shaped composite parts while meeting manufacturing cost specifications. The approach involves using limited experimental tests and theory-guided machine learning (TGML). The method's iterative solution scheme is presented in Figure 4. The TGML method is comprised of two main phases: Initialization and Optimization. The following subsections describe the workflow deployed in each phase.

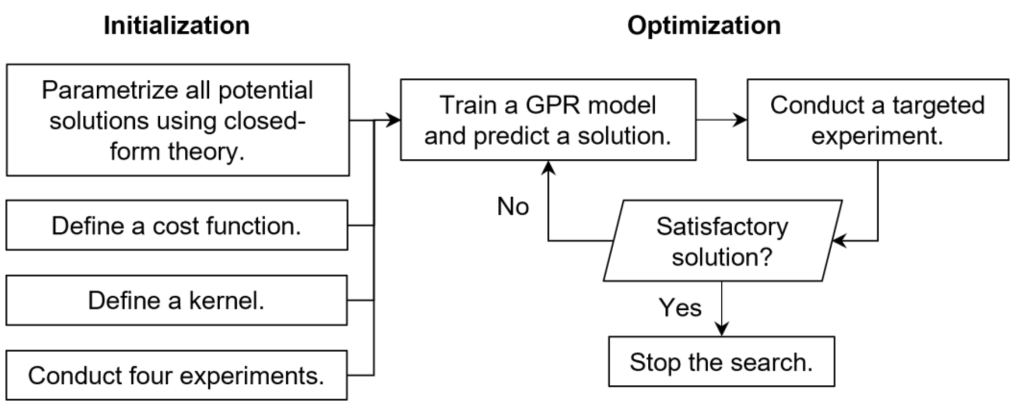

Figure 4. Theory-guided machine learning methodology for finding an optimal solution (i.e., cure cycle) to minimize PIDs and satisfy cost specifications.

The first step of the TGML method's Initialization phase is constructing a design architecture consisting of parametrized potential solutions. In this work, potential solutions include two-stage (i.e., "two-hold", "two step", etc.) cure cycles, wherein all cycles include a variable first stage and a fixed second stage consisting of a temperature hold and cool-down equal to 180 °C for 120 minutes and 2.78 °C/min, respectively (Figure 5). The second-stage temperature and cool-down values were chosen based on the manufacturer's recommended cure cycle (MRCC) for the T800S/3900-2B material system [11], to ensure a final degree of cure of about 90%. The MRCC consists of heating from 20 to 180 °C at 2 °C/min, holding at 180 °C for 120 minutes, then cooling the system down at 2.78 °C/min.

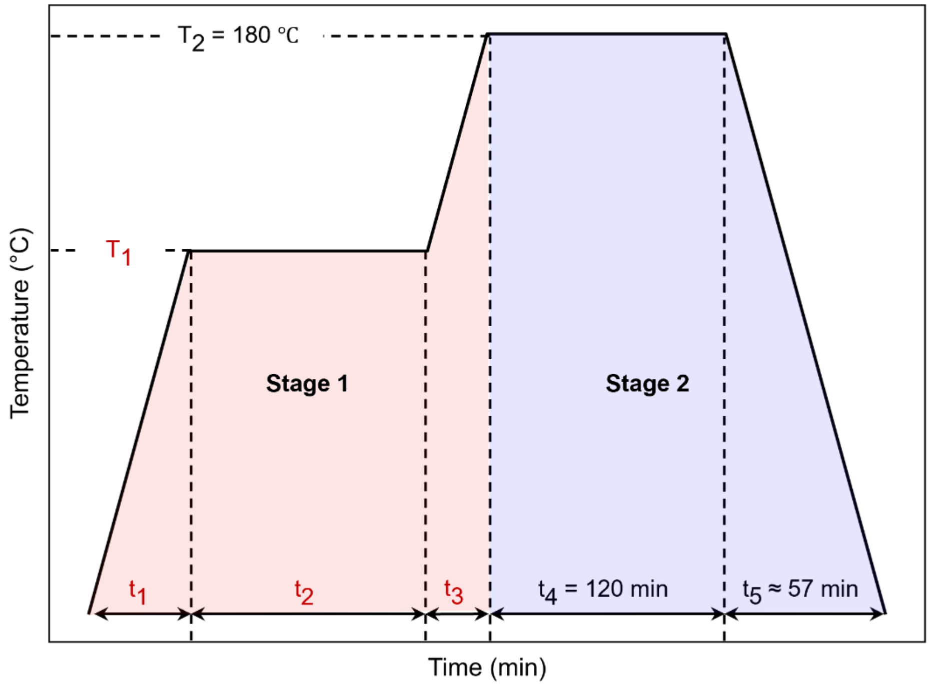

Figure 5. Generalized temperature profile of a two-stage cure cycle with a variable first stage and a fixed second stage.

The first stage of a cure cycle may be described by four main parameters: first heat-up time (t_1), hold temperature (T_1), hold time (t_2), and second heat-up time (t_3). By setting constraints or potential values for these parameters, a wide range of evaluable solutions can be generated. In this work, six values for T_1 (120, 130, 140, 150, 160, 170 °C) and t_2 (900, 600, 420, 300, 240, 180 min) were used as parameters for potential hold temperatures and times. The choice of potential hold times was based on the time for complete vitrification to occur ($T_g > T + 28$ °C) at each value of T_1 [14,15]. Additionally, values for t_1 and t_3 were determined by constraining ramp rates to 2, 4, and 8 °C/min for the first heat-up and 0.1, 2, 4, and 8 °C/min for the second heat-up. Consequently, by defining three potential first ramp rates, six hold temperatures, six hold times, and four second ramp rates, a total of $3 \times 6 \times 6 \times 4 = 432$ possible cure cycles were defined to be considered as potential optimization solutions in this study.

After the list of potential solutions was constructed, closed-form theory was used to generate two additional parameters to describe each of the 432 cycles. First, the evolution of T800S/3900-2B's glass transition and the temperature at which vitrification occurs (T_{vit}) during each cycle were calculated [15]. The vitrification temperature has been demonstrated to be highly influential in the development of process-induced residual stresses and deformations in similar thermosetting composite materials [16]. Considering the presence of thermoplastic tougheners in T800S/3900-2B, the state in which these particles are in during processing may also play a critical role in residual stress and PID levels. Therefore, to include the effects of thermoplastic tougheners in the additional cure cycle parameters, the glass transition temperature of the particles ($T_{g,tp}$), assumed as 150 °C [17], was subtracted from each T_{vit} value for every cycle. Thus, the fifth parameter to describe each cycle was set equal to $T_{vit} – T_{g,tp}$.

The sixth and final parameter to describe each potential cycle was meant to acknowledge the presence of devitrification ($T > T_g$), which may also play a critical role in residual stress developments. Following the cure kinetics model used for T_{vit} calculations [15], cycles exhibiting no devitrification were assigned a value of 0, while cycles experiencing devitrification were labeled with a parameter of 1. Thus, at the completion of the parametrization phase, a list of 432 potential solutions was constructed, each with a unique combination of six parameters determined using closed-form theory: t_1, T_1, t_2, t_3, $T_{vit} – T_{g,tp}$, and 0 or 1 corresponding to devitrification.

The next step of the Initialization phase consisted of defining a function to quantify the cost of each cure cycle in terms of deformation and manufacturing time (i.e., cycle time). In this work, the total cost of each cure cycle was set equal to

$$Cost = \frac{A + (K - A)}{C + Qv \times exp^{-B(\delta - M)}} + L\delta - B + 0.1t \tag{1}$$

where δ is the deformation of the L-shaped parts, t is the total cycle time, A (0) and K (1000) are the lower and upper bounds of a sigmoid function, B (0.1866) and M (0) are the sigmoid function's growth rate and midpoint, v (0.2229), Q (1), and C (1) are constants which affect the steepness of the sigmoid function's transitions, and L (1) is the slope of a linear function,. In nonmathematical terms, Equation 1 states that the total cost of each cycle is exponential-linearly dependent on the deformation of L-shaped parts, and linearly dependent on total cycle time. A plot of the defined cost as a function of deformation and cycle time is shown in Figure 6.

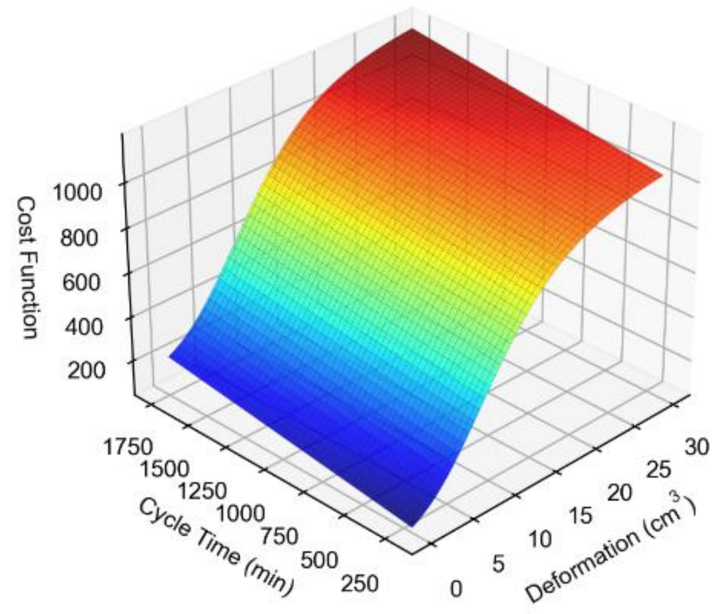

Figure 6. Custom cost function used for cure cycle optimization to minimize PIDs in L-shaped parts.

After the cost function was defined, a kernel was selected to be used for GPR training and optimization. For this work, a combination of linear and Matern ($\nu = 2.5$) kernels was used to describe the covariance between datapoints [18]. This combination allowed for the complexity of the cost function to be captured while maintaining generalizability and minimizing the risk of overfitting.

The final step of the Initialization phase was to conduct four experiments. The temperature profiles (T), simulated glass transition temperatures of the thermoset ($T_{g,ts}$) and thermoplastic ($T_{g,tp}$), and degree of cure (DoC) for each cycle are shown in Figure 7. Cycle 1 consisted of heating from 20 to 120 °C at 2 °C/min, holding at 120 °C for 900 minutes, heating to 180 °C at 0.1 °C/min, holding at 180 °C for 120 minutes, then cooling to room temperature. Cycle 2 consisted of heating from 20 to 150 °C at 2 °C/min, holding at 150 °C for 300 minutes, heating to 180 °C at 2 °C/min, holding at 180 °C for 120 minutes, then cooling to room temperature. Cycle 3 consisted of heating from 20 to 120 °C at 4 °C/min, holding at 120 °C for 900 minutes, heating to 180 °C at 4 °C/min, holding at 180 °C for 120 minutes, then cooling to room temperature. Cycle 4 consisted of heating from 20 to 120 °C at 8 °C/min, holding at 120 °C for 420 minutes, heating to 180 °C at 8 °C/min, holding at 180 °C for 120 minutes, then cooling to room temperature. The simulated vitrification temperatures for Cycles 1, 2, 3, and 4 were 120, 150, 120, and 180 °C, respectively. Devitrification occurred in Cycles 2 and 3 but did not occur in Cycles 1 and 4. The four cycles used during GPR initialization were chosen because they offer a wide range of diverse training parameters, as listed in Table I.

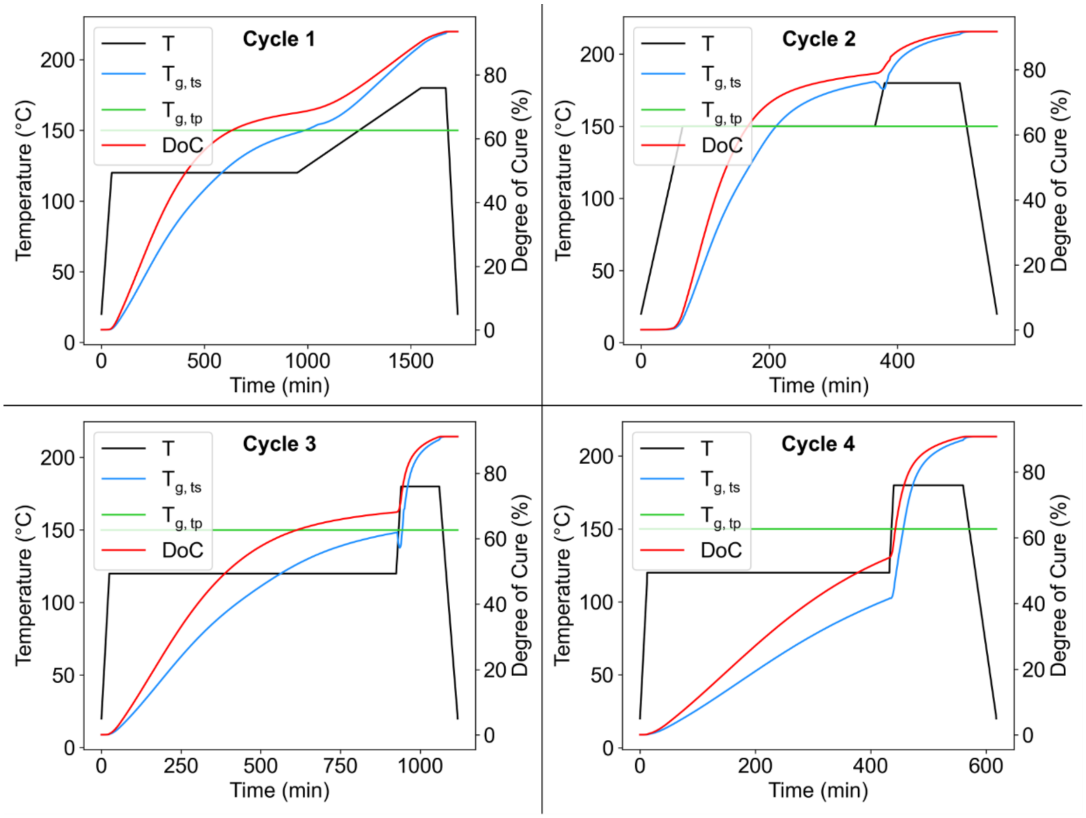

Figure 7. Temperature profile (T), glass transition temperature of the thermoset ($T_{g,ts}$) and thermoplastic ($T_{g,tp}$), and degree of cure (DoC) for the four initial tests.

TABLE I. CURE CYCLE PARAMETERS FOR THE FIRST FOUR EXPERIMENTS

Cycle	**t_1 (min)**	**T_1 (°C)**	**t_2 (min)**	**t_3 (min)**	**$T_{vit} – T_{g,tp}$ (°C)**	**Devitrification? (0 = No, 1 = Yes)**
1	50	120	900	600	-30	0
2	35	150	300	15	0	1
3	25	120	900	15	-30	1
4	12.5	120	420	7.5	30	0

Finally, after four experiments and initial training of the GPR model, deformation values were predicted for each of the 432 cure cycles in the first step of the TGML’s Optimization phase. Next, a targeted experiment was conducted with parameters for which the GPR model predicted an optimal solution. As previously mentioned, the optimal solution in this work was a cure cycle that produced the lowest average deformation and cost less (i.e., according to the custom cost function) than the one-hold MRCC. Then, after one targeted experiment, the GPR model was retrained with the updated experimental results and produced a new prediction for an optimal solution. Finally, experiments were conducted and the GPR model was retrained until an optimal solution predicted by GPR was validated experimentally.

RESULTS AND DISCUSSION

Figure 8 shows the spatial profiles and flange spring-in of one L-shaped composite part cured during the four initial tests. The profile and spring-in of the tool and a composite part cured according to the one-hold MRCC are also included in the figure for comparison purposes. Cycle 1 produced an average flange corner spring-in of 0.59°, a flange tip spring-in of 0.76°, a maximum flange warpage of 0.23 mm, and a deformation of 15.72 cm^3. Cycle 2 produced an average flange corner spring-in of 0.61°, a flange tip spring-in of 0.91°, a maximum flange warpage of 0.11 mm, and a deformation of 18.5 cm^3. Cycle 3 produced an average flange corner spring-in of 0.67°, a flange tip spring-in of 1.06°, a maximum flange warpage of 0.11 mm, and a deformation of 21.4 cm^3. Cycle 4 produced an average flange corner spring-in of 0.74°, a flange tip spring-in of 1.34°, a maximum flange warpage of 0.20 mm, and a deformation of 26.3 cm^3. The relative deformation, time, and total cost of each cycle are compared to results obtained for the one-hold MRCC in Figure 9, which were obtained in previous experiments. Points in the plot represent average measurements from the three manufactured parts, while error bars correspond to the standard deviation within each measurement set.

The results in Figure 8 and Figure 9 entice two discussion-worthy points. First, Cycle 4, which caused vitrification to occur at the highest temperature of 180 °C, showed to significantly elevate PID levels in the L-shaped composite parts. These findings reinforce results obtained in previous studies on similar materials, showing a direct link between vitrification temperature and deformation [16]. Secondly, the profile and deformation measurements from Cycle 1 showed that PIDs may be significantly reduced by adding lower-temperature intermediate holds into a cure cycle. For example, during Cycle 1, the material vitrified at 120 °C and exhibited a reduction in deformation of approximately 10 %.

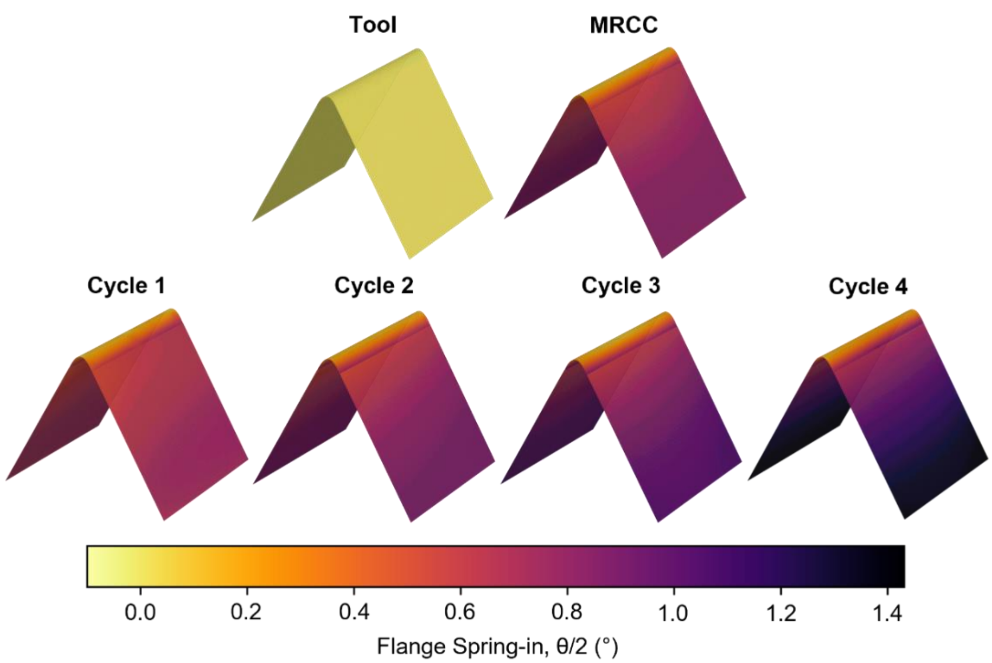

Figure 8. Spatial profiles and flange spring-in of L-shaped composite parts cured according to the first four GPR training cycles. The profiles and spring-in of the tool and part cured according to the one-hold MRCC cycle are also shown to be used as reference.

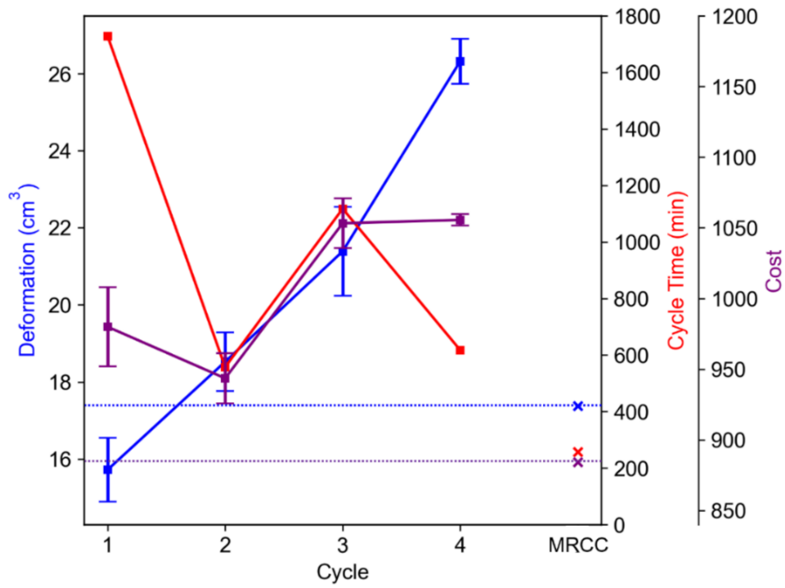

Figure 9. Deformation, cycle time, and cost of first four experiments compared to values obtained from one-hold MRCC cycle.

Although Cycle 1 demonstrated a significant reduction in deformation, the total cost of the cycle remained higher than the MRCC due to the relatively long cycle time. These results indicated that the optimal solution had not been achieved in the four training tests, and that initializing a GPR search was the necessary next step to conduct following the TGML method. Thus, using the six parameters listed in Table I and the experimental costs of each of the four training cycles, the GPR model predicted the smallest cost and deformation for the following sequence of parameters: t_1 = 32.5 min, T_1 = 150 °C, t_2 = 300 min, t_3 = 300 min, $T_{vit} – T_{g,tp}$ = 0 °C, and Devitrification = 0. This sequence equates to the cycle illustrated in Figure 10, labeled and referenced as Cycle 5 through the remainder of this paper. Cycle 5 consisted of heating from 20 to 150 °C at 4 °C/min, holding at 150 °C for 300 minutes, heating to 180 °C at 0.1 °C/min, holding at 180 °C for 120 minutes, then cooling to room temperature.

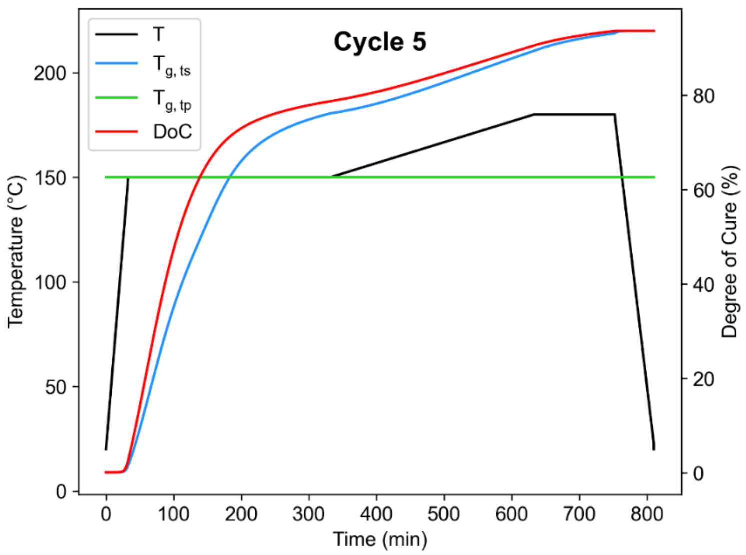

Figure 10. Temperature profile (T), glass transition temperature of the thermoset ($T_{g,ts}$) and thermoplastic ($T_{g,tp}$), and degree of cure (DoC) for the first GPR targeted test.

Figure 11 shows the spatial profile and flange spring-in of one L-shaped composite part cured according to the first GPR targeted test. Cycle 5 produced an average flange corner spring-in of 0.69°, a flange tip spring-in of 0.75°, a maximum flange warpage of 0.24 mm, and a deformation of 15.7 cm^3. The relative deformation, cycle time, and total cost of Cycle 5 are compared to the training tests and MRCC results in Figure 12. Compared with the MRCC test, the first targeted cycle showed a lower deformation value. These results demonstrate that the GPR algorithm successfully provided parameters for a cure cycle with reduced PIDs after just four training tests. However, the total cost of the first targeted cycle remained slightly higher than the MRCC's due to the relatively long cycle time.

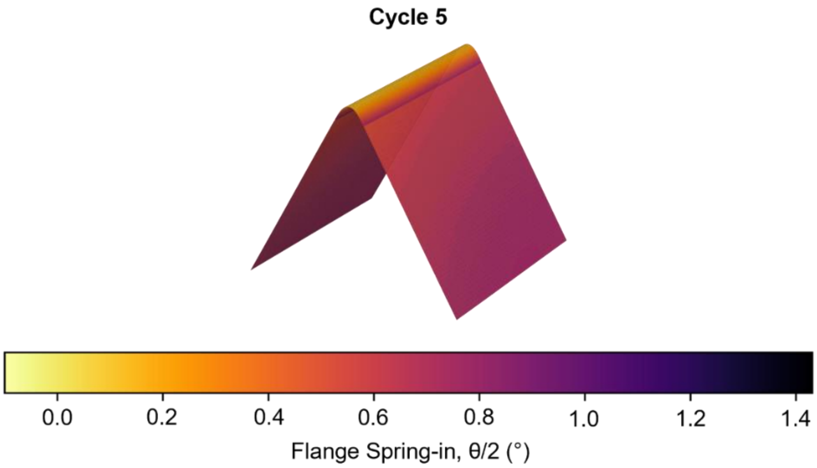

Figure 11. Spatial profile and flange spring-in of an L-shaped composite part cured according to the first GPR targeted cycle.

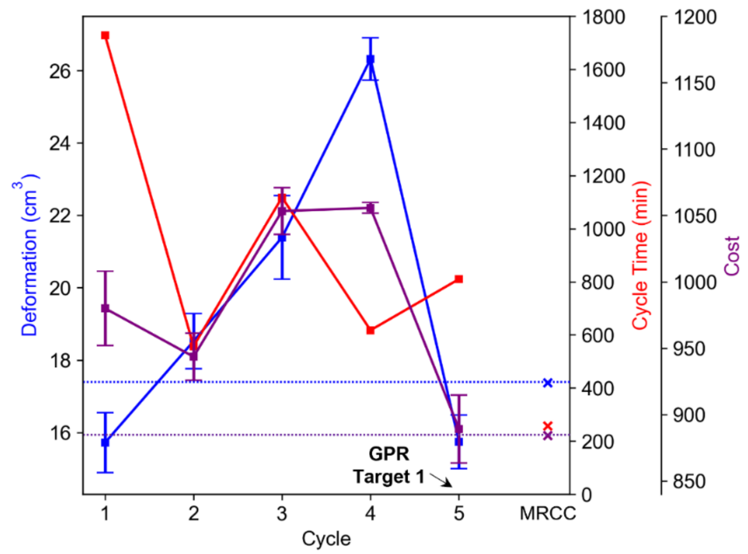

Figure 12. Deformation, cycle time, and cost of first GPR targeted test compared with the initial training tests and MRCC values.

Since the cost constraints had not been reached after one targeted cycle, the GPR model was retrained with updated experimental results, consisting of four training and one targeted test. After retraining, the GPR model predicted the smallest cost and deformation for the following sequence of parameters: t_1 = 75 min, T_1 = 170 °C, t_2 = 180 min, t_3 = 2 min, $T_{vit} - T_{g,tp}$ = 20 °C, and Devitrification = 0. This sequence equates to the cycle illustrated in Figure 13, labeled and referenced as Cycle 6 through the remainder of this paper. Cycle 6 consisted of heating from 20 to 170 °C at 2 °C/min, holding at 170 °C for 180 minutes, heating to 180 °C at 2 °C/min, holding at 180 °C for 120 minutes, then cooling to room temperature.

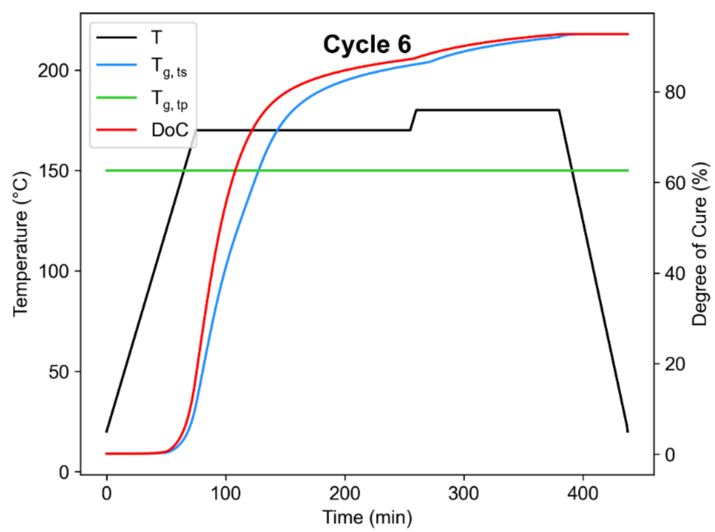

Figure 13. Temperature profile (T), glass transition temperature of the thermoset ($T_{g,ts}$) and thermoplastic ($T_{g,tp}$), and degree of cure (DoC) for the second GPR targeted test.

Figure 14 shows the spatial profile and flange spring-in of one L-shaped composite part cured according to the second GPR targeted test. Cycle 6 produced an average flange corner spring-in of 0.64°, a flange tip spring-in of 0.84°, a maximum flange warpage of 0.11 mm, and a deformation of 16.7 cm^3. The relative deformation, cycle time, and total cost of Cycle 6 are compared to the training tests and MRCC results in Figure 15. Compared with the MRCC test, the second targeted cycle showed a lower deformation and cost. In other words, the GPR algorithm converged to an optimal solution after four initial and two targeted experiments guided by theory. Following the TGML methodology, the search for an optimal cure cycle to reduce PIDs could then be concluded.

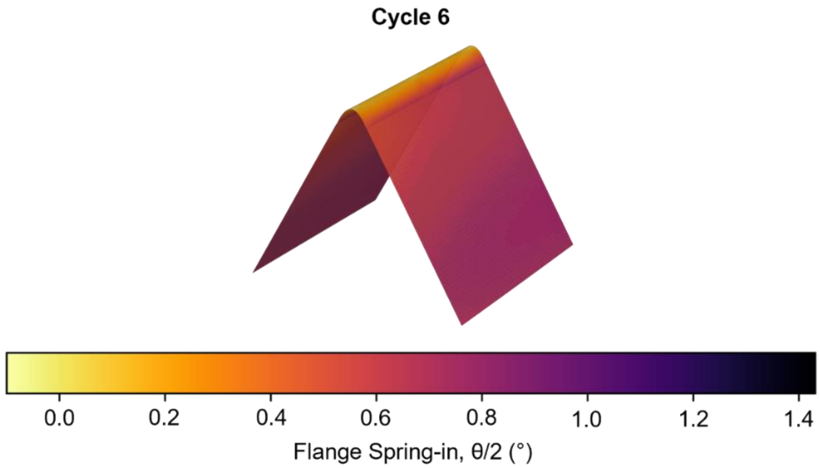

Figure 14. Spatial profile and flange spring-in of an L-shaped composite part cured according to the second GPR targeted cycle.

doi.org/10.12783/asc38/36531

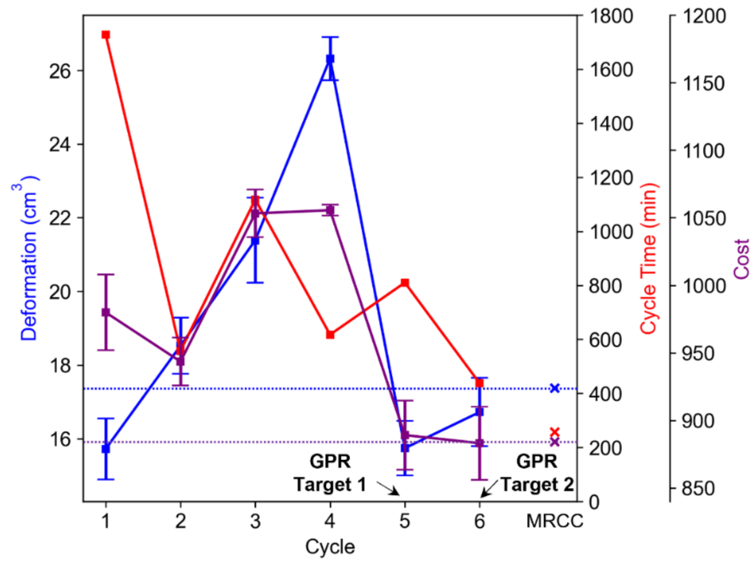

Figure 15. Deformation, cycle time, and cost of second GPR targeted test compared with the initial training tests, first GPR targeted test, and MRCC values.

SUMMARY AND CONCLUSIONS

This study aimed to demonstrate a theory-guided machine learning (TGML) method to find an optimal cure cycle to minimize process-induced deformation in L-shaped composite (T800S/3900-2B) parts while satisfying cost constraints. An iterative methodology was proposed, consisting of limited experimental tests and Gaussian Process Regression (GPR) guided by closed-form theory. The TGML procedure is generalizable and may be used to efficiently minimize spring-in, warpage, and/or volumetric deformation in composite laminates. Following the TGML method in this study, a two-stage cure cycle that reduces volumetric deformation and defined cost compared to a traditional one-stage cycle was discovered and validated after four initial and two targeted experiments. The main conclusions from this work are as follows:

- Process-induced deformations (PIDs) in L-shaped T800S/3900-2B parts depend highly on the cure cycle used during processing. In this study, two-stage temperature cycles containing single vitrification points at 120, 150, or 170 °C reduced PIDs by up to 10% compared to the one-stage Manufacturer's Recommended Cure Cycle (MRCC). On the other hand, two-stage temperature cycles containing a single vitrification point at 180 °C or multiple vitrification points can enhance PID levels by over 150%.
- Using closed-form theory to guide Gaussian Process Regression (GPR) models can be an effective optimization strategy to minimize PIDs in composite parts, and potentially contribute to solving other science and engineering problems.

ACKNOWLEDGEMENTS

This work was supported by Toray Composite Materials America, Inc.

REFERENCES

[1] Zobeiry, N., and A. Poursartip. 2015. "The Origins of Residual Stress and Its Evaluation in Composite Materials," in *Structural Integrity and Durability of Advanced Composites*, Woodhead Publishing, pp. 43–72.

[2] Zobeiry, N., A. Forghani, C. Li, K. Gordnian, R. Thorpe, R. Vaziri, G. Fernlund, and A. Poursartip. 2016. "Multiscale Characterization and Representation of Composite Materials during Processing," *Phil. Trans. R. Soc. A*, 374: 20150278.

[3] Fernlund, G., C. Mobuchon, and N. Zobeiry. 2018. "2.3 Autoclave Processing," in *Comprehensive Composite Materials II*, Amsterdam: Elsevier, pp. 42–62.

[4] Li, C., N. Zobeiry, K. Keil, S. Chatterjee, and A. Poursartip. 2014. "Advances in the Characterization of Residual Stress in Composite Structures," presented at SAMPE Conference, June 2-5, 2014.

[5] Albert, C., and G. Fernlund. 2002. "Spring-in and Warpage of Angled Composite Laminates," *Compos. Sci. Technol.*, 62(14): 1895–1912.

[6] Karpatne, A., G. Atluri, J.H. Faghmous, M. Steinbach, A. Banerjee, A. Ganguly, S. Shekhar, N. Samatova, and V. Kumar. 2017. "Theory-Guided Data Science: A New Paradigm for Scientific Discovery from Data," *IEEE Trans. Knowl. Data. En.g*, 29(10): 2318–2331.

[7] Zobeiry, N., J. Reiner, and R. Vaziri. 2020. "Theory-Guided Machine Learning for Damage Characterization of Composites," *Compos. Struct.*, 246: 112407.

[8] Zobeiry, N., and K.D. Humfeld. 2021. "A Physics-Informed Machine Learning Approach for Solving Heat Transfer Equation in Advanced Manufacturing and Engineering Applications," *Eng. Appl. Artif. Intell.*, 101: 104232.

[9] Zobeiry, N., S. Profile, and A. Poursartip. 2019. "Theory-Guided Machine Learning Composites Processing Modelling for Manufacturability Assessment in Preliminary Design," presented at NAFEMS 17th World Congress, June 17-20, 2019.

[10] Liao, Z., C. Qiu, J. Yang, J. Yang, and L. Yang. 2022. "Accelerating the Layup Sequences Design of Composite Laminates via Theory-Guided Machine Learning Models," *Polymers*, 14(15): 3229.

[11] "3900 Prepreg System | Toray Composite Materials America, Inc." 2020. Available: https://www.toraycma.com/3900-prepreg-system/.

[12] Odagiri, N., H. Kishi, and M. Yamashita. 1996. "Development of TORAYCA Prepreg P2302 Carbon Fiber Reinforced Plastic for Aircraft Primary Structural Materials," *Adv. Compos. Mater.*, 5(3): 249–254.

[13] Van Rossum, G., and J.F. Drake. 2021. "Python. Version 3.10."

[14] "Composite Materials Handbook, Volume 1. Polymer Matrix Composites Guidelines for Characterization of Structural Materials | Department of Defense," 2002.

[15] Dykeman, D. 2008. "Minimizing Uncertainty in Cure Modeling for Composites Manufacturing," Doctor of Philosophy Thesis, University of British Columbia, Vancouver.

[16] White, S. R., and H.T. Hahn. 1993. "Cure Cycle Optimization for the Reduction of Processing-Induced Residual Stresses in Composite Materials," *Journ. Compos. Mater.*, 27(14): 1352-1378.

[17] Chen, C., A. Poursartip, and G. Fernlund. 2021. "Influence of the Glass Transition of Interlaminar Particles on Shear Behaviour during Cure of Interlayer Toughened Thermoset Composites," *Compos. Part A Appl. Sci. Manuf.*, 147: 106447.

[18] Tipping, M. E. 2003. "Bayesian Inference: An Introduction to Principles and Practice in Machine Learning," *Lecture Notes in Artificial Intelligence Subseries of Lecture Notes in Computer Science*, O. Bousquet, U. von Luxburg, and G. Rätsch, eds., pp. 41–62.